ORIGINAL ARTICLE

Numerical study of asymmetric and axisymmetric thermal jet with entropy generation concept

D. Belakhal[1,2], K. Rahmani[2], A. Elkaroui[3], S. Ben Haj Ayech[3], N. Mahjoub Said [4,5] and B. Imine[6]

[1] University of science and technology of Oran- PO Box 1505 - El Mnaouer in the City of Oran- Algeria
Phone: +213699647576

[2] Research Laboratory Modeling Simulation and Optimization of Real Complex Systems, group: Mechanical Systems and New Energies at the University of Djelfa, Algeria

[3] LGM, National Engineering School of Monastir at the University of Monastir, Tunisia

[4] LGM, Preparatory Institute for Engineering Studies at the University of Monastir, Tunisia

[5] Departments of Physics, College of Science, King Khalid University, Abha 61413, Saudi Arabia

[6] Laboratory of Aeronautics and Propulsive Systems, University of science and technology of Oran, PO Box 1505, El Mnaouer in the City of Oran, Algeria

ABSTRACT – In the current investigation, numerical study of a thermal jet of asymmetric (rectangular and elliptical) and axisymmetric (circular) geometry was investigated with variable density to verify the impact of the ratio of density and geometry on the generation of entropy. The central jet was brought to different temperatures (194, 293 and 2110 K) to obtain density ratios (0.66, 1 and 7.2) identical to a mixture jet (($Air-CO_2$), ($Air-Air$) and ($Air-He$)), respectively. Solving the three-dimensional numerical resolution of the Navier Stocks for turbulent flow permanent enclosed on the turbulence model K-εstandard was made. The results acquired are compared with that carried out in previous experimental studies, where it was concluded that, the axisymmetric (circular) geometry increases the entropy generation.

INTRODUCTION

Numerous studies indicated the importance of the asymmetric jets in improving the capacity of burners by increasing the combustion efficiency and reducing the emanation of pollutants [1]. This is because it had the ability to increase and improve the efficacy of mixing aggressively and exposes a higher retention rate than circular ones [2]. The results of other works also conducted on the turbulent jet of variable density [3–5], confirmed that the mixture efficiency increases when the ratio of density increases. And, the experimental work of Mesnier [6] explained the impact of density variation and geometry of the outlet section on the mixing process of vertical subsonic turbulent jets. As of an examination of the dynamic field with Particular Image Velocimetry (PIV) in the vertical planes, he indicated on the impact of the injection rate and also the role of the density ratio on the jet. Ellipsoidal and rectangular jets greatly improve the entrainment rate. He observed a creation of turbulent structures closest to the outlet with the elliptical jet with the rectangular and circular jet. Furthermore, the consequence of other studie indicated that the jet's nozzle engineering plays crucial and final role in contributing the augment of noise reduction technique [7].

Recently, researchers have studied the notion of generation of entropy and highlighted its main role in fluid flow processes. Where, Gazzah and Belmabrouk [8] used two turbulence closing models to study a turbulent jet with a co-current of air; they concluded that the second-order model predicts a lower value of entropy generation better than the first-order model. After, they accomplished a numerical investigation in a round and hot turbulent jet with entropy generation[9]; they succeeded in showing that the temperature augment in the hot air jet at the inlet and the velocity augment in the co-current induce an improvement in the rate of generation entropy and the mixture performance. Also, they studied the impact of the directed co-current on the rate of generation of local entropy in a turbulent and hot round jet [10].They indicated that the orientation of the co-current to a positive angle improves the efficacy of the mixing and augment the rate of generation of local entropy. In the same context, El Karoui et al [11] have studied numerically a turbulent plane jet with variable density; they came to the conclusion that the rate of generation of local entropy gradually increases, eventually reaching an approximate value when the temperature of the inlet jet increases. As well, they carried another numerical investigation in a hot turbulent jet within the co-current [12]. The main results obtained indicated that,the efficiency of jet mixing, the quantity of entrained air and the rate of generation of total entropy reduces when the velocity of the co-current increases. For their part, Boussoufi et al [13] have studied numerically the flow characteristics and entropy generation of multiple jets and succeeded in showing that, the multiple jets augments the rate of generation entropy. It was also studied by Morsli et al [14–18] and others differently in several areas. Where their results indicated that the rates of generation of total entropy reduce with an augment equivalent ratio and oxygen percentage in air [14], augment with Rayleigh number [15] and in position where reactions are effective [16]. Additionally, Ries et al [17] studied the production of entropy in the turbulent flow near the wall inside a general heat exchanger from air to air, where

---

they came to the conclusion that entropy production is primarily through viscous dissipation rather than heat transfer processes. Also, Pirkandi et al [18] found that the rate of entropy generation of the fuel cell cycle is superior than in the chiller cycle and water pumps.

The aim of the present work is concentrated on the impact of nozzle geometry and varying the density on the generation of entropy, Basing on numerically developing of an asymmetric (rectangular and elliptical) and axisymmetric (circular) thermal jet with a variable density, drowning in a mobile and confined atmosphere. Noteworthy, that the central jet was exposed to different temperatures (194, 293 and 2110 K) to obtain density ratios (0.66, 1 and 7.2) identical with a mixture jet ((Air-CO_2), (Air-Air) and (Air-He)),this jet was generated using a tube of a nearly similar section, with rectangular, elliptical and circular shapes. The dimensional geometry is present in Figure 1. In this study, solving the Navier Stocks for turbulent flow permanent enclosed by the turbulence model with standard two equations K-ε is made by the finite volume method.
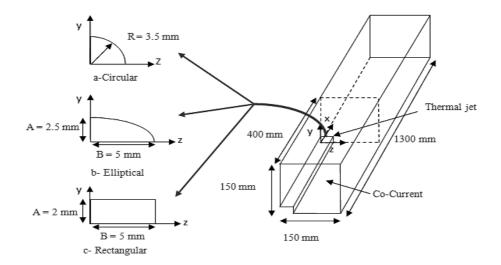

Figure 1. Geometric configurations. *a, b* and *c*, corresponding the thermal jet injector

CONSERVATION EQUATION AND TURBULANCE MODEL

The variable density turbulent jet is a single-phase and *3D* flow of Newtonian fluid; it can be considered as a perfect gas, which means that the Stokes hypothesis is verified [2]. The principal equations were formulated and proposed by Favre [19] with a mass-weighted average [2].

Favre- Averaged Mass- Conservation Equation:

$$\frac{\partial}{\partial x_j}\left(\bar{\rho}\widetilde{U_j}\right) = 0 \tag{1}$$

Favre- Averaged Momentum- Conservation Equation:

$$\frac{\partial}{\partial x_j}\left(\bar{\rho}\widetilde{U_i}\widetilde{U_j}\right) = \bar{\rho}g_i - \frac{\overline{\partial P}}{\partial X_i} - \frac{\partial}{\partial X_i}\left(\overline{\rho U_i'' U_j''}\right) + \frac{\partial}{\partial X_j}\left[\bar{u}\left(\frac{\partial \widetilde{U_i}}{\partial X_j} + \frac{\partial \widetilde{U_j}}{\partial X_i}\right) - \frac{2}{3}\bar{u}\frac{\partial \widetilde{U_k}}{\partial X_k}\delta_{ij}\right] \tag{2}$$

Favre- Averaged Energy- Conservation Equation:

$$\frac{\partial}{\partial x_j}\left(\bar{\rho}\widetilde{T}\widetilde{U_j}\right) = \frac{\partial}{\partial X_j}\left(\frac{\lambda}{C_P} \times \frac{\partial T}{\partial X_j}\right) + \frac{\partial}{\partial X_j}\left(\overline{\rho t'' U_j''}\right) \tag{3}$$

Equation of State:

$$\bar{\rho} = PM/R\widetilde{T} \tag{4}$$

where R isthe constant of ideal gas, M: the molecular mass for the gas, and P is the ambient pressure, which in the current case is the atmospheric pressure.

Standard *k-ε* Model

The turbulence k-ε standard model with two equation (kinetic energy Eq. (8) and dissipation rate Eq. (9)), the Reynolds constraints Eq. (5) and the Reynolds heat flux vector Eq. (6) were given by the following relations[12].

$$\left(\overline{\rho u_i'' u_j''}\right) = -\mu_t \left(\frac{\partial u_i}{\partial x_j} + \frac{\partial u_j}{\partial x_i}\right) + \frac{2}{3}\bar{\rho}\, k\, \delta_{ij} \tag{5}$$

$$\left(\overline{\rho t'' U_j''}\right) = -\frac{\mu_t}{\sigma_t} \times \frac{\partial T}{\partial x_j} \tag{6}$$

where μ_t is the turbulent viscosity, δ_{ij} is the Kronecker symbol δij= 1 if $i = j$, 0 if not, k is the kinetic turbulent energy, and C_μ *is* a constant. The quantity μ_t is distinct by the following expression [12].

$$\mu_t = C_\mu \rho \frac{k^2}{\epsilon} \tag{7}$$

Equation of the kinetic turbulent energy:

$$\bar{\rho}\frac{\partial}{\partial X_j}(u_j k) = \frac{\partial}{\partial X_j}\left(\left(\mu + \frac{u_t}{\sigma_k}\right)\frac{\partial k}{\partial X_j}\right) + P_k - \bar{\rho}\varepsilon \tag{8}$$

Equation of turbulence dissipation rate:

$$\bar{\rho}\frac{\partial}{\partial X_j}(u_j \varepsilon) = \frac{\partial}{\partial X_j}\left(\left(\mu + \frac{u_t}{\sigma_\varepsilon}\right)\frac{\partial \varepsilon}{\partial X_j}\right) + \frac{\varepsilon}{k}(C_1 P_k - C_{\epsilon 2}\bar{\rho}\varepsilon) \tag{9}$$

where P_k is the average production of turbulent energy (k) expressed in the form [12]:

$$P_k = \mu_t \left(\frac{\partial u_i}{\partial x_j} + \frac{\partial u_j}{\partial x_i}\right)\frac{\partial u_i}{\partial x_j} \tag{10}$$

The turbulence model constants are[12]: $C_{\varepsilon 1}$=1.44, $C_{\varepsilon 2}$=1.92, C_μ=0.09, σ_k=1 and σ_ε =1.3.

Entropy Generation Rate

In this section, the effect of density and geometry on the entropy generationis studied by the second theorem of thermodynamics [12]. As the temperature and velocity fields are known, it then becomes possible to calculate the rate of volumetric entropy production at every point of the fluid in the following way[12]:

$$\dot{s}_{gen} = \left(\dot{s}_{gen}\right)_{heat} + \left(\dot{s}_{gen}\right)_{frict} \tag{11}$$

$$\left(\dot{s}_{gen}\right)_{heat} = \frac{\lambda_{eff}}{T^2}\left\{\left(\frac{\partial T}{\partial x}\right)^2 + \left(\frac{\partial T}{\partial y}\right)^2 + \left(\frac{\partial T}{\partial z}\right)^2\right\} \tag{12}$$

$$\left(\dot{s}_{gen}\right)_{frict} = \begin{cases} \frac{1}{2}\left(\frac{\mu_{eff}}{T}\right)\left\{\left(\frac{\partial u}{\partial x}\right)^2 + \left(\frac{\partial v}{\partial y}\right)^2 + \left(\frac{\partial w}{\partial z}\right)^2 + \\ 2\left(\left(\frac{\partial u}{\partial z} + \frac{\partial w}{\partial x}\right)^2 + \left(\frac{\partial u}{\partial y} + \frac{\partial v}{\partial x}\right)^2 + \left(\frac{\partial v}{\partial z} + \frac{\partial w}{\partial y}\right)^2\right)\right\} \end{cases} \tag{13}$$

where, λ_{eff} , μ_{eff} are, the thermal conductivity and the dynamic viscosity effective for the fluid [13], respectively. $\left(\dot{s}_{gen}\right)_{frict}$ and $\left(\dot{s}_{gen}\right)_{heat}$ are the components of viscous and thermal generation of entropy [13].

NUMERICAL METHOD

The system under study consists of a thermal air jet (very hot, isothermal or cold), generated inside a tube an axisymmetric (circular) and asymmetric (rectangular and elliptical) section of diameter *Dj*, the jet moves with velocity *Uj*. This jet develops inside an air co-current that passes through a square section tube, 300 mmside, at a velocity *Ua*. Table 1 presents the variables of the cases under study. A quarter of the physical domain of the problem under consideration is explained in Figure 1. The Gambit mesh creation software was used for the put on show of the geometry and generation of the mesh. The simulation was executed out by the ANSYS Fluent calculation code. In this study, solving the Navier Stocks for turbulent flow permanent enclosed by the turbulence model with standard two equations $k - \varepsilon$, is made by the finite volume method. The treatment of pressure-speed coupling problems was affected by the SIMPLE

algorithm. It is important to know that the solution is considered to be convergent when the residue is fewer than 10^{-6}. The Reynolds (Re) number and density ratio ($R\rho$) values have existed in the Table 1.

Table 1. The variables of the cases under study

		Tj (k)	Ta (k)	Uj (m/s)	Ua (m/s)	Dj [mm]	Da [mm]	Re	Rρ
Circular	Cold	194	293	40	0.36	7	300	34500	0.66
	Isothermal	293	293	40	0.36	7	300	19200	1
	Very hot	2110	293	60	0.62	7	300	3600	7.2
Rectangular	Cold	194	293	40	0.36	7.13	300	34500	0.66
	Isothermal	293	293	40	0.36	7.13	300	19200	1
	Very hot	2110	293	60	0.62	7.13	300	3600	7.2
Elliptical	Cold	194	293	40	0.36	7.071	300	34500	0.66
	Isothermal	293	293	40	0.36	7.071	300	19200	1
	Very hot	2110	293	60	0.62	7.071	300	3600	7.2

RESULTS AND DISCUSSION

Grid Independency Test

The mesh quality and resolution play are of major importance in the numerical solution accuracy and stability[13]. Thus, many meshes were tested to observe that the simulation results are independent of the mesh refinement level. The tested meshes of cells: grid 1 (550,000), grid 2 (750,000), and grid 3 (950,000), are displayed in the figures below. Note that network sensitivity test 1 gives results similar to two from network 2 and 3. Therefore, using network (1) at 550,000 cells is sufficient to improve calculation time, memory size, and obtain a network-independent digital solution.
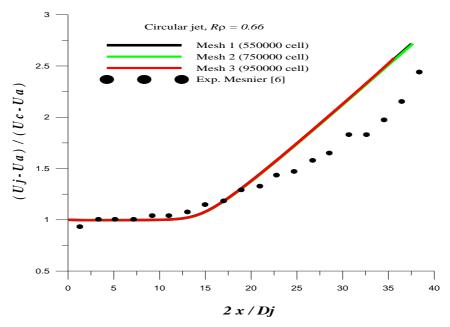

Figure 2. Axial evolution of *(Uj-Ua) / (Uc-Ua)* the longitudinal velocity along the axis of circular jet, for three different meshes
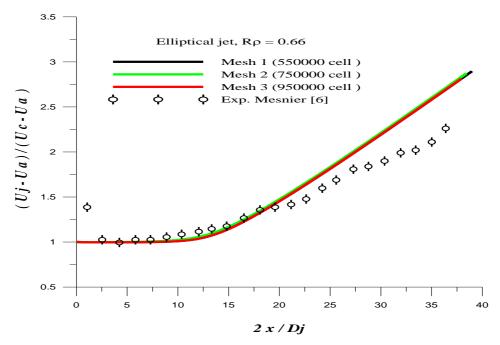
Figure 3. Axial evolution of *(Uj-Ua) / (Uc-Ua)* the longitudinal velocity along the axis of an elliptical jet, for three different meshes
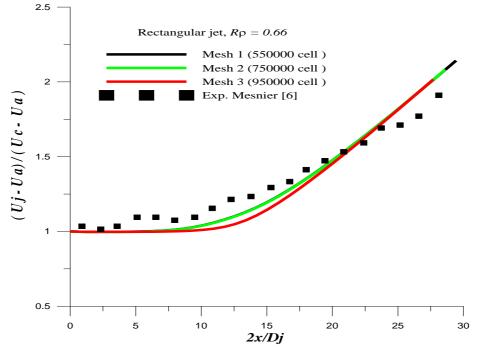

Figure 4. Axial evolution of *(Uj-Ua) / (Uc-Ua)* the longitudinal velocity along the axis of rectangular jet, for three different meshes

Impact of the Geometry Nozzle

At a density ratio ($R\rho = 0.66$), the impact of the geometry nozzle on the normal longitudinal velocity *(Uj-Ua) / (Uc-Ua)*, is studied in Figure 5. For all cases, the centerline velocity profile is separated by two regions: constant velocity region for *x/Dj* lower than 6 and increasing region for *x/Dj* greater than 6. In the first region, the length for the potential core is shorter concerning an asymmetric jet and the centerline velocity is equalize to the inlet velocity for all configurations [2], in the second region, the axial evolution of the longitudinal velocity concerning the jet asymmetric (rectangular and elliptical) is slightly higher than that obtained concerning the jet axisymmetric (circular)[2]. This maybe attributed to the fact that grand aspect ratio jets influence the axis reversal phenomenon. It is also important to observe the axial variation of the longitudinal velocity for a rectangular jet is slightly larger than in connection with an elliptic one because rectangular jets possess the advantages of grand aspect ratio (ellipsoidal jets and angular jets)[1], The results

acquired in this case are in good agreement with those reported by Mesnier [6] and Imine et al [2]. These findings confirm the reciprocity of Sanders et al[20] hypothesis, which consists of replacing the study of temperature by that of the mass fraction.
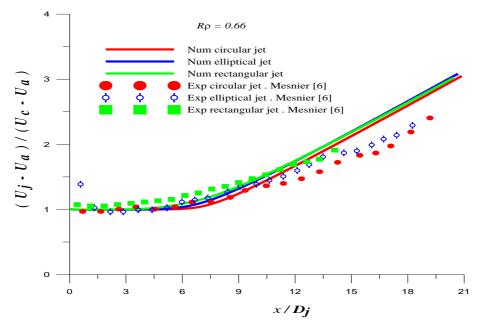

Figure 5. Impact of the geometry nozzle on (Uj- Ua) / (Uc-Ua) the normal longitudinal velocity, with a density ratio Rρ = 0.66

Entropy Generation

The evolution of the generation of local entropy per volume unit for the three configurations versus the normalized distance x / Dj, for a density ratio $R\rho = 0.66$ is present in Figure 06. It turned out that when the normalized distance x / Dj is fewer than 2.5; the generation of local entropy per unit of volume Neglected since there are no velocity and temperature gradients[13]. When x / Dj is in the distance between 2.5 to 8, strong velocity gradients are caused by turbulent disturbances; these it's enhance the rapid augment in the rate of generation of local entropy per unit of volume [9]. Where, three peaks observed for the axial distances x / Dj = 5.5, 6.5 and 7.5.These correspond to the following injector geometries (rectangular geometry ($\dot{s} = 800 \, w / m^3 K$), elliptical geometry ($\dot{s} = 1000 \, w / m^3 K$) and circular geometry ($\dot{s} = 1250 \, w / m^3 K$)), respectively. Where, the profiles reach the maximum then start decreasing more quickly concerning an asymmetric jet in comparison with concerning an axisymmetric jet. After these, the generation of local entropy per unit of volume remains constant [13]for all three types of jets. Viscous dissipation becomes negligible [11, 15].
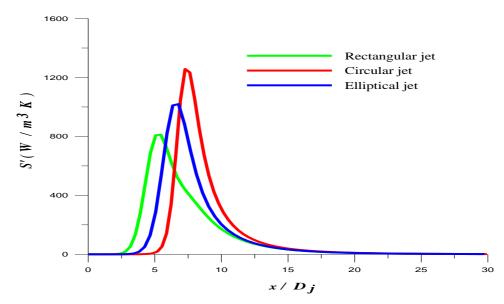

Figure 6. The evolution of generation of local entropy by volume unit along the axis, for the three configurations

Contours of the Entropy

The contours of generation of local entropy by volume unit, for the three injector geometries under study, are existed in Figure 7 with density ratios ($R\rho = 0.66$). Note that the contour lines are very crowded close to the outlet of the nozzle and have elevated values, as well, the layer of the mixture augments straight with the direction of the jet and, the temperature gradient gradually reduces in the section of the affinity of the jet [11,15]. This means that the viscous dissipation at the outlet of the nozzle is predominant but gets negligible in the region of the affinity of the jet [11,15]. In the regions near the outlet of the nozzle in the asymmetric and axisymmetric jets, it is observable that the generation of local entropy by volume unit values are large when the jet is axisymmetric (circular) compared to the other case (jet asymmetric (rectangular and elliptical)).
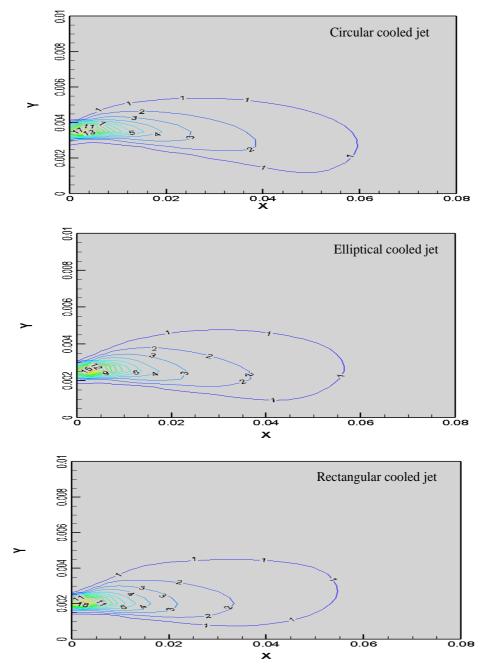

Figure 7. The contours of the generation of local entropy by volume unit for different injector geometries, for the cooling jet ($R\rho = 0.66$)

Contours of the Entroy

The contour lines of generation of local entropy volumetric for diverse values of the inlet jet density ratio $R\rho$ (0.66, 1 and 7.2) are present in Figure 8. For these values, the generation of local entropy volumetric contours are very dense and of grand values nigh the nozzle outlet, however it is negligible elsewhere [11,15]. This is certainly due to the different

density ratio values.Where, the mixture layer expands in the direction of the jet. And its expansion and the values of generation of local entropy volumetric are higher at (very hot jet *(Rρ =7.2)*) compared to the other two cases (cold jet (*Rρ = 0.66*) and isothermal jet (*Rρ = 1*)).This is consistent with the results of the references [11,13].
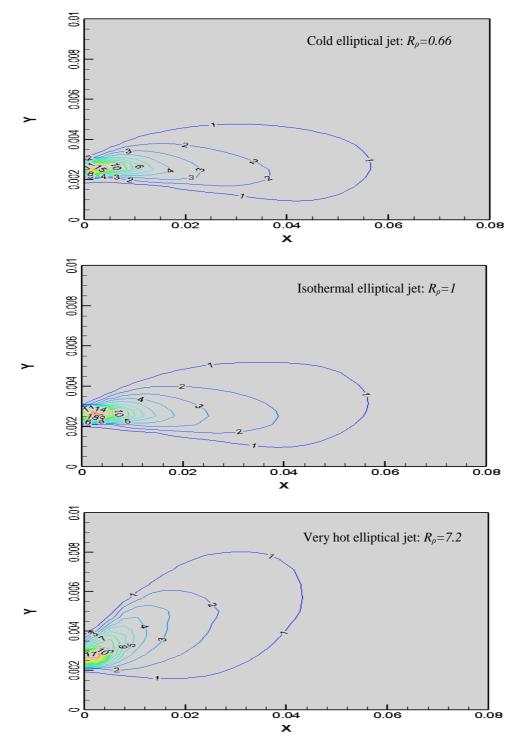

Figure 8. The contours of the generation of local entropy by volume unit for different density ratios, for the elliptical jet

CONCLUSION

This work concentrated on the numerical study of non-circular (rectangular and elliptical) thermal jets with variable density using a first order *K-ε* standard turbulence model allowed drawing the following conclusions:

- The CFD predictions of this study are reasonably in good accord with the experimental results relating to mixing jets, which confirms the hypothesis that a thermal jet can be replaced by a mixing jet;

- The axial evolution of the longitudinal velocity close to the asymmetric jet (rectangular and elliptical) is somewhat greater than that obtained concerning the axisymmetric jet (circular) which promotes the exchange of energy between the jet and the co-flow atmosphere and especially in the highly heated jet;

- The obtained numerical results indicated that the generation of local entropy per unit of volume is high near the exit of the nozzle, but unimportant in the section of the affinity of the jet. In addition, it is greater concerning an injector with axisymmetric geometry compared to asymmetric geometry.

- The grand values of generation of local entropy per unit of volume correspond to a high density ratio of the jet.

REFERENCE

[1]   V. Faivre, "Etude experimentale et numerique du controle actif de jets dans des chambres de combustion," Institut National Polytechnique De Toulouse, 2003.

[2]   B. Imine, O. Imine, M. Abidat, A. Liazid, "Study of non-reactive isothermal turbulent asymmetric jet with variable density," *Computational Mechanics*, vol. 38, no. 2, pp. 151–162, 2006, doi: 10.1007/s00466-005-0727-9.

[3]   J. Pagé, "Contribution à l'étude des jets turbulentsaxisymétriques à masse volumique variable," Université d'Orléans., 1998.

[4]   M. Senouci, A. Bounif, "Simulation numérique d'un jet turbulent axisymétrique à masse volumique variable par le modele au second ordre (RSM)," *MEC Industries*, vol. 12, pp. 315–324, 2011, doi: 10.1051/meca/2011105.

[5]   A. Moutte, "Etude de jets turbulents à masse volumique variable : impact de la variation de masse volumique sur la structure fine et le mélange," Ecole Centrale de Marseille, 2018.

[6]   B. Mesnier, "Études sur le développement de jets turbulents à masse volumique variable, à géométries axisymétrique et asymétrique," Universite D'Orleans, 2001.

[7]   H. H. Assoum, J. Hamdi, K. Abed-Meraïm, M. El Hassan, A. Hammoud, A. Sakout, "Experimental investigation the turbulent kinetic energy and the acoustic field in a rectangular jet impinging a slotted plate," *Energy Procedia*, vol. 139, pp. 398–403, 2017, doi: 10.1016/j.egypro.2017.11.228.

[8]   M. H. Gazzah and H. Belmabrouk, "Evaluation des Modèles de Turbulence dans un Jet Turbulent Débouchant dans un Co-courant d ' Air : Concept de Génération d ' Entropie," *International Journal of Science, Engineering and Technology*, vol. 3, no. 2, pp. 84–88, 2015.

[9]   M. H. Gazzah and H. Belmabrouk, "Local entropy generation in co-flowing turbulent jets with variable density," *International Journal of Numerical Methods for Heat & Fluid Flow*, vol. 24, no. 8, pp. 1679–1695, 2014, doi: 10.1108/HFF-02-2013-0055.

[10]   M. H. Gazzah and H. Belmabrouk, "Directed co-flow effects on local entropy generation in turbulent heated round jets," *Computers & Fluids*, vol. 105, pp. 285–293, 2014, doi: 10.1016/j.compfluid.2014.09.037.

[11]   A. Elkaroui, M. H. Gazzah, N. M. Saïd, P. Bournot, G. Le Palec, "Entropy generation concept for a turbulent plane jet with variable density," *Computers & Fluids*, vol. 168, pp. 328–341, 2018, doi: 10.1016/j.compfluid.2017.01.003.

[12]   A. Elkaroui, S. B. H. Ayech, M. H. Gazzah, N. M. Saïd, G. Le Palec, "Numerical study of local entropy generation in a heated turbulent plane jet developing in a co-flowing stream," *Applied Mathematical Modelling*, vol. 62, pp. 605–628, 2018, doi: 10.1016/j.apm.2018.06.020.

[13]   M. Boussoufi, A. Sabeur-Bendehina, A. Ouadha, S. Morsli, M. El Ganaoui, "Numerical analysis of single and multiple jets," *The European Physical Journal Applied Physics*, vol. 78, no. 3, 2017, doi: 10.1051/epjap/2017170039.

[14]   S. Morsli, A. Sabeur, M. El Ganaoui, "Numerical simulation of entropy generation in hydrogen-air burner," *Fluid Dynamics and Materials Processing*, vol. 11, no. 4, pp. 342–353, 2015, doi: 10.3970/fdmp.2015.011.342.

[15]   S. Morsli, A. Sabeur, M. El Ganaoui, H. Ramenah, "Computational simulation of entropy generation in a combustion chamber using a single burner," *Entropy*, vol. 20, no. 12, 2018, doi: 10.3390/e20120922.

[16]   S. Morsli, A. Sabeur, M. El Ganaoui, "Influence of aspect ratio on the natural convection and entropy generation in rectangular cavities with wavy-wall," *Energy Procedia*, vol. 139, no. December, pp. 29–36, 2017, doi: 10.1016/j.egypro.2017.11.168.

[17]   F. Ries, Y. Li, A. Sadiki, "Entropy production in near-wall turbulent flow inside a generic air-to-air plate heat exchanger," 2018.

[18]   J. Pirkandi, A. M. Joharchi, M. Ommian, "Thermodynamic and exergic modelling of a combined cooling, heating and power system based on solid oxide fuel cell," *Journal of Mechanical Engineering Science*, vol. 13, no. 4, pp. 6088–6111, 2019.

[19]   A. Favre, L. S. . Kovasznay, R. Dumas, J. Gaviglio, M. Coantic, *la turbulence en mécanique des fluides: bases théoriques et expérimentales, méthodes*. 1976.

[20]   H. Sanders, B. Sarh, I. Gokalp, "Etude numérique des jets turbulents à température élevée," *Rev. Générale Therm.*, vol. 35, pp. 232–242, 1996.